JOURNAL OF CATALYSIS 131, 22–35 (1991)

CO Oxidation over Pd and Cu Catalysts

IV. Prereduced Al_2O_3-Supported Copper

KYUNG I. CHOI AND M. ALBERT VANNICE[1]

Department of Chemical Engineering, Pennsylvania State University, University Park, Pennsylvania 16802

Received December 4, 1990; revised February 26, 1991

A study of the kinetics for CO oxidation over supported, prereduced Cu crystallites showed that it is close to first order in CO and near zero order in O_2 at temperatures around 400 K. *In situ* IR measurements under reaction conditions revealed a clear first-order dependence on chemisorbed CO and an absence of activity when no adsorbed CO was detected; thus an Eley–Rideal mechanism is eliminated and a Langmuir–Hinshelwood surface reaction between adsorbed CO molecules and chemisorbed oxygen is strongly supported. These Cu/Al_2O_3 catalysts were more active than Pd/Al_2O_3 catalysts, and the average turnover frequency of 0.016 s^{-1} at 400 K and 26 Torr CO was about four times higher than the average value on Pd. An invariant IR band at 2118 cm^{-1} for CO was very near that of 2115 cm^{-1} reported for CO adsorbed on an oxidized Cu(111) surface and therefore was consistent with the near-saturation oxygen coverage indicated from the kinetic behavior. Analysis of the IR spectra at various temperatures allowed a heat of adsorption of 7.2 kcal/mol to be determined under reaction conditions. An activation energy of 22–27 kcal/mol was estimated for the rate-determining step, i.e., the surface reaction, which is somewhat higher than that reported for adsorbed CO and submonolayer coverages of oxygen on Cu single crystals.

INTRODUCTION

Although Jones and Taylor reported in 1923 that copper is an active catalyst for the reaction between CO and O_2 (*1*), only one additional kinetic study at higher pressure (near atmospheric) has been conducted with metallic Cu (*2*) and no specific activities have been reported for either supported or unsupported Cu. However, the interaction of CO with preadsorbed oxygen on the three low-index crystal planes of Cu has been studied by Ertl (*3*) and Habraken *et al.* (*4–7*). They found little difference in the activity on these low-index surfaces, which suggested that the reaction was structure insensitive. In contrast, in a recent study of Cu surfaces by Arlow and Woodruff it was proposed that structural sensitivity may exist for this reaction because they observed the highest reaction rates on surfaces containing both steps and low-index terraces (*8*). All of these Cu single-crystal studies have found that high oxygen coverages retard the reaction rate and that a surface reaction between an adsorbed CO molecule and an oxygen atom occurs, thus indicating the presence of a Langmuir–Hinshelwood mechanism.

Because oxygen adsorbs much more strongly than CO on Cu, high oxygen coverages typically exist and reaction rates are lower on these oxygen-covered Cu surfaces. Consequently, it might be assumed that higher reaction temperatures are necessary to obtain the same degree of activity using Cu oxide catalysts and, indeed, cupric oxide exhibits activities per unit surface area similar to those of noble metal catalysts, such as Pt, at auto exhaust temperatures (around 713 K) (*9*). Prokopowicz *et al.* have studied CO oxidation at 523 K over a silica-supported cupric oxide catalyst (*10*), and they observed a first-order dependency on CO, which is a characteristic of base metals (*11*),

[1] To whom correspondence should be sent.

0021-9517/91 $3.00

and a zero-order dependency on O_2 above 4% O_2 (*10*). This agreed with the results of Schwab and Drikes (*12*) and those of Miro *et al.* for a sintered CuO/mordenite catalyst (*13*); however, Prokopowicz *et al.* proposed an Eley–Rideal reaction mechanism between gas-phase CO molecules and adsorbed oxygen atoms (*10*). Huang *et al.* recently studied cupric oxide supported on γ-Al_2O_3, found that the activity for CO oxidation depended strongly on the pretreatment, and concluded that the reaction is structure sensitive (*14*). In contrast to this behavior, Garner *et al.* have reported a first-order dependence on O_2 and a zero-order dependence on CO over bulk cuprous oxide (*15, 16*).

Unfortunately, the state of the copper/copper oxide surface under reaction conditions was not probed in these investigations. This study was conducted to gain a better understanding of the CO oxidation reaction over a prereduced Cu/Al_2O_3 catalyst by determining the kinetic behavior at higher partial pressures and by simultaneously using *in situ* IR spectroscopy before and during reaction to monitor the CO species present on the surface. This also provided a comparison of catalytic behavior with Pd/Al_2O_3 and bimetallic $Pd–Cu/Al_2O_3$ catalysts under the same reaction conditions (*17, 18*). In addition, the appropriateness of a Langmuir–Hinshelwood reaction sequence could be examined, and turnover frequencies could be measured for this reaction on copper for the first time. This paper discusses these results.

EXPERIMENTAL

The alumina support was δ-Al_2O_3 (W. R. Grace Co., 138 m^2/g) and the metal precursor was $CuCl_2$ (99.999% Aldrich Chemical Co.). Before preparation of these catalysts, the δ-Al_2O_3 was ground and sieved to a 40/80-mesh size and then calcined in dry air (825 cm^3/min) at 723 K for 2.5 h. Catalyst preparation involved an incipient wetness method based upon established methods (*19*). After impregnation of the δ-Al_2O_3 with the $CuCl_2$ solution, the catalyst was air-dried in an oven overnight at 393 K and then calcined at 673 K in dry air (825 cm^3/min) for 2 h to provide a 12 wt% Cu/δ-Al_2O_3 catalyst.

The catalyst was reduced *in situ* in the adsorption cell or the reactor using the following procedure: the sample was exposed to flowing He (30 cm^3/min) at 300 K; then the temperature was increased to 573 K and held there for 1 h. The He flow was switched to H_2 (30 cm^3/min) and the catalyst was reduced for 3 h at 573 K followed by treatment in flowing He (30 cm^3/min) for an hour at the same temperature before cooling to 300 K. A standard volumetric chemisorption method (*19*) was used for the measurement of hydrogen and CO chemisorption at 195 and 300 K. Sample preparation, equipment, and data acquisition methods were the same as those described previously (*20*). For the XRD experiment with the reduced sample following CO chemisorption measurements, the catalyst was loaded into a leakproof holder inside a N_2-purged dry box.

RESULTS

The kinetic behavior of this supported, prereduced Cu/Al_2O_3 catalyst is summarized in Table 1, and Arrhenius plots from samples in each reactor system are shown in Fig. 1. No deactivation was observed during these runs. Specific activities in the form of a turnover frequency (TOF = molecules $site^{-1}$ s^{-1}) are also included, and they are computed from the irreversible uptake of CO at 195 K assuming an adsorbed CO molecule defines a site. (If the adsorption stoichiometry of CO_{ad}/Cu_s = 0.5 reported by Chesters and Pritchard were assumed (*21*), then all TOFs would be one-half as large.) All chemisorption results for either fresh or used samples are listed in Table 2. Partial pressure dependencies were first determined by fitting a power rate law to the data shown in Fig. 2, which were obtained from 0.4 to 52 Torr for CO and from 16 to 84 Torr for O_2. Over the prereduced 12% Cu/δ-Al_2O_3 catalyst at 403 K in the IR reactor, the partial pressure

TABLE 1

Kinetic Behavior for CO Oxidation over Prereduced Cu/δ-Al_2O_3

Catalyst (12% Cu/δ-Al_2O_3)	E_{app}[a] (kcal/mol)	Activity[a] at 400K (μmol/g cat s)	TOF[a,b] at 400 K (s^{-1})	Partial pressure dependency[c]	
				X	Y
Microreactor	17.1 ± 0.4	0.64	0.017	—	—
IR reactor	21.6 ± 1.6	0.76	0.014	0.7	0

[a] Standard reaction conditions: P_{O_2} = 132 Torr, P_{CO} = 26 Torr, total pressure = 750 Torr. Uncertainties represent 95% confidence limits.

[b] Turnover frequency (molecules CO $site^{-1}$ s^{-1}) based on an adsorbed CO molecule at 195 K representing a site (used sample).

[c] $r = kP_{CO}^{X} P_{O_2}^{Y}$ at 403 K. P_{CO} = 26 Torr when Y was obtained. P_{O_2} = 132 Torr when X was obtained.

dependency on CO was 0.7, which is consistent with previous trends for base metal catalysts (*12*), while the dependency on O_2 was near zero, as shown in Table 1. The activation energies were 21.6 kcal/mol from the IR reactor study and 17.1 kcal/mol from the kinetic study in the microreactor, as shown in Table 1 and Fig. 1.

At 303 K in He, IR spectra were obtained at various CO concentrations, as shown in Fig. 3. With CO in He, an IR spectrum with a CO band at 2118 cm^{-1} was obtained at 0.4 Torr and this peak continuously increased in size, with no change in position, as the CO partial pressure was increased. At the standard reaction conditions of 132 Torr O_2 and 26 Torr CO, the CO band again did not change its position but the intensity decreased as the temperature increased, as shown in Fig. 4. Comparing the IR spectrum obtained at 26 Torr CO in Fig. 3 with that obtained at 303 K in Fig. 4, the intensity of

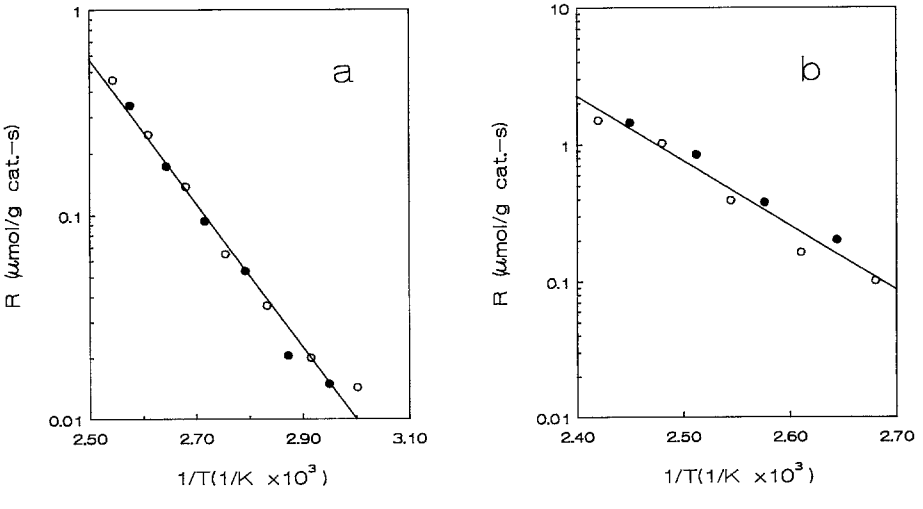

FIG. 1. Arrhenius plots for prereduced 12% Cu/δ-Al_2O_3. Total pressure = 750 Torr, P_{CO} = 26 Torr, P_{O_2} = 132 Torr, balance was He. Open symbols, ascending temperature; closed symbols, descending temperature. (a) Microreactor. (b) IR reactor system.

TABLE 2

Chemisorption Results for 12% $Cu/\delta\text{-}Al_2O_3$

Sample	Chemisorbed Gas	Temperature (K)	Irreversible uptake (μmol/g cat)
I (fresh)	H_2	300	0
	CO	300	19[a]
	CO	195	24
II (fresh)	H_2	300	0.5
	CO	300	26[a]
	CO	195	28
III (fresh)	H_2	300	0.5
	CO	300	23[a]
	CO	195	23
After use in the microreactor	CO	300	17.5[a]
	CO	195	38
After use in the IR reactor cell	CO	300	58[a]
	CO	195	55

[a] Total uptake on Cu.

the 2118 cm^{-1} band was reduced by one-third in the presence of 132 Torr O_2; therefore, it can be concluded that adsorbed oxygen blocks CO adsorption on the Cu surface, in agreement with the single-crystal studies conducted at much lower pressures (*3–7*).

During the partial pressure runs for CO and O_2, the IR spectra in Figs. 5 and 6 were obtained. At the lowest CO concentrations (less than 0.6 Torr CO), no CO band at 2118 cm^{-1} was observed, as shown in Fig. 5. This is another indication that adsorbed oxygen

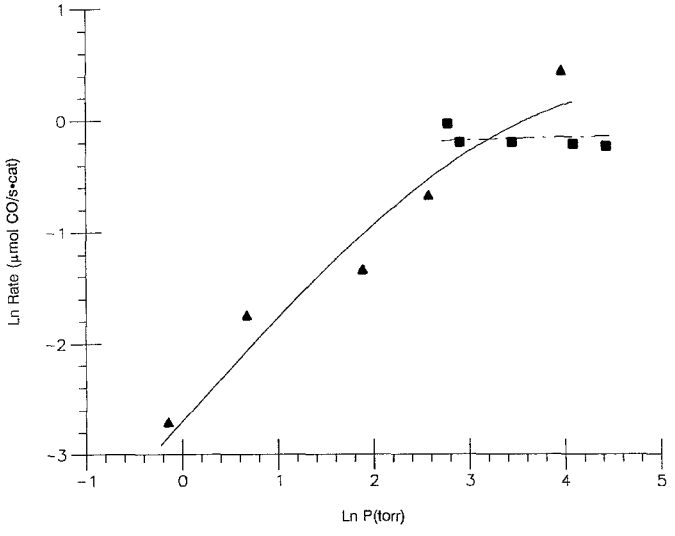

FIG. 2. Partial pressure dependencies on CO (▲) and O_2 (■) for CO oxidation at 403 K over prereduced 12% $Cu/\delta\text{-}Al_2O_3$: Gas flow = 28.5 cm^3/min, total pressure = 750 Torr, P_{CO} = 26 Torr when P_{O_2} varied, P_{O_2} = 132 Torr when P_{CO} varied (IR reactor). Curves represent predicted rates from the Langmuir–Hinshelwood expression in Eq. (5).

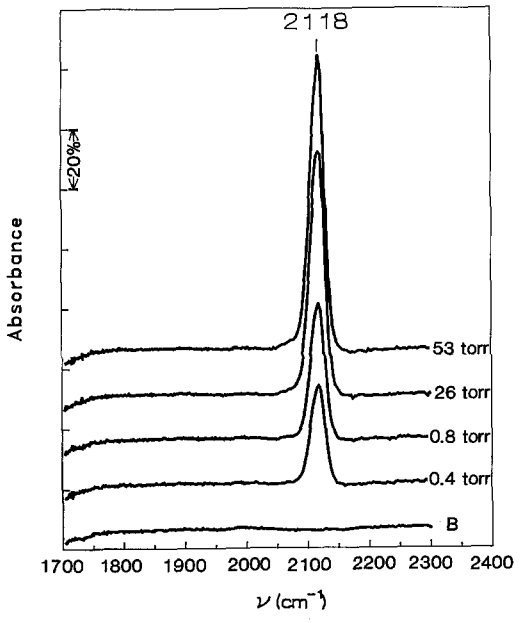

FIG. 3. IR spectra of CO adsorbed on prereduced 12% $Cu/\delta\text{-}Al_2O_3$ at 303 K and increasing CO pressures. Gas flow = 28.5 cm^3/min, total pressure = 750 Torr, balance was He.

reduces CO adsorption because a strong CO band on the initial Cu surface was observed at these CO partial pressures, as shown in Fig. 3. A very small peak began to appear at 0.9 Torr CO, and its intensity continuously increased as the CO pressure was increased. The activity for CO_2 formation also increased simultaneously with an increase in the intensity of this peak. It is noteworthy that no detectable activity was observed until this CO band was detected. These two results provide overwhelming support for a Langmuir–Hinshelwood (L-H) mechanism, as discussed later, and they clearly eliminate an Eley–Rideal mechanism. As the O_2 pressure was reduced from 84 to 16 Torr during the O_2 partial pressure run, the intensity of the 2118 cm^{-1} peak increased about 15–20%, as shown in Fig. 6, and the activity also showed a very small 10–20% increase (Fig. 2). This trend is again consistent with the assumption that CO molecules adsorbed on the surface are required for the CO oxidation reaction because oxygen adsorbed at these high coverages hinders the adsorption of CO.

After the partial pressure runs, the catalyst was reduced again at 573 K for 3 h and IR spectra were obtained under 26 Torr CO in He, as shown in Fig. 7. At 303 K the peak intensity, now at 2115 cm^{-1}, was so strong that it was off scale. This intensity had not existed when the CO spectra were obtained after the initial 3-h reduction, as shown in Fig. 3. Therefore, CO adsorption had increased after the CO oxidation reaction was conducted and the catalyst was subjected to an additional reduction step. Several authors have reported an increase in Cu surface area in Cu/Al_2O_3 catalysts after aging in oxygen and reduction in CO (*22–25*); thus, a similar process presumably occurred with this 12% $Cu/\delta\text{-}Al_2O_3$ catalyst during the CO oxidation reaction. However, it is also possible that if the sample were not completely reduced after the initial reduction step, the second 3-h reduction could have increased the amount of reduced surface copper. This

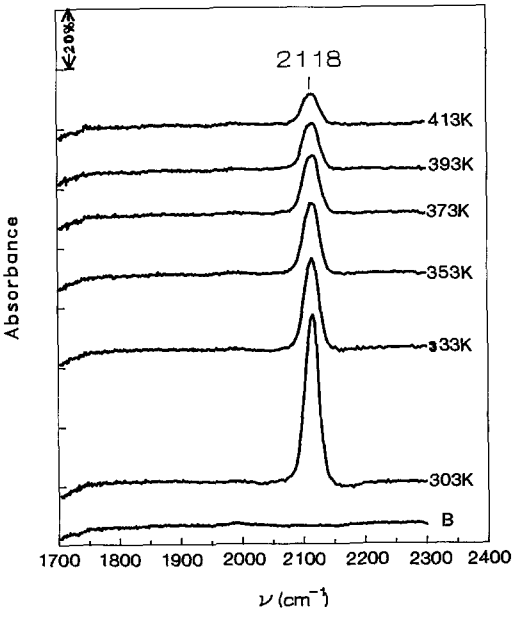

FIG. 4. IR spectra of CO adsorbed on prereduced 12% $Cu/\delta\text{-}Al_2O_3$ at standard reaction conditions and increasing temperature. Gas flow = 28.5 cm^3/min, total pressure = 750 Torr, P_{CO} = 26 Torr, P_{O_2} = 132 Torr, balance was He.

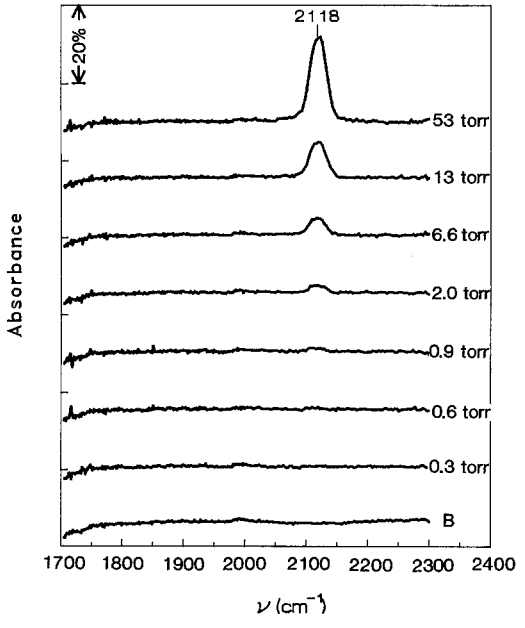

FIG. 5. IR spectra of CO adsorbed on prereduced 12% Cu/δ-Al_2O_3 during the CO partial pressure run. Gas flow = 28.5 cm^3/min, total pressure = 750 Torr, P_{O_2} = 132 Torr, balance was He, T = 403 K.

enhancement of CO uptake was also detected by CO chemisorption, as shown in Table 2. Over the fresh reduced 12% Cu/δ-Al_2O_3 catalyst, an average irreversible uptake value of 25 μmol CO/g cat was obtained at 195 K and an average total uptake value of 23 μmol CO/g cat occurred at 300 K; however, higher uptakes of 55 μmol CO/g cat at 195 K and 58 μmol CO/g cat at 300 K were obtained on the used catalyst taken from the IR reactor. Note that the CO uptakes represent irreversible adsorption at 195 K but total (irreversible + reversible) uptake at 300 K.

DISCUSSION

Pritchard and co-workers (*21, 26–32*) have studied not only the structure of adsorbed CO but also the vibrational spectra of CO molecules on different Cu single-crystal surfaces using a reflection–adsorption IR technique, and their results are collected in Table 3. The (100) and (111) planes give single bands near 2080 cm^{-1} at low coverages, and these bands shift slightly to higher wavenumbers on the (100) plane and to lower ones on the (111) plane with increasing CO coverage. The latter behavior is unusual in that it is in the direction opposite that observed for increasing CO coverages on Pd and other noble metals (*29*). However, with Cu this decrease in frequency also occurs on the (110), (311), and (755) planes for the higher-wavenumber band, and it also occurs for CO adsorption on Ag (*33*), another group IB metal. Grimley (*34*) has suggested that electronic interactions of adsorbed molecules through a metal substrate can lead to strengthened or weakened adsorption depending on the distance of separation. The (110) plane gives rise to two absorption bands at low coverage which merge together at high coverage. The one band at 2088 cm^{-1} is not very different in wavenumber from that of CO on the (100) plane, but the other one at 2104 cm^{-1} is notably higher. Similar pairs of absorption bands are found at low coverage on the (211), (311), and (755) planes, and these

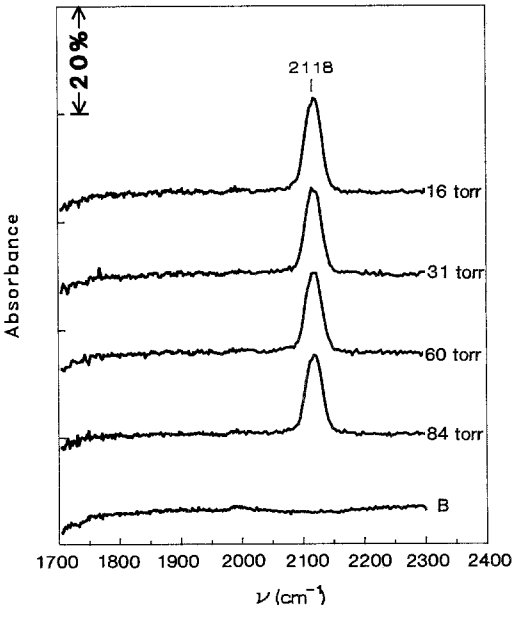

FIG. 6. IR spectra of CO adsorbed on prereduced 12% Cu/δ-Al_2O_3 during the O_2 partial pressure run. Gas flow = 28.5 cm^3/min, total pressure = 750 Torr, P_{CO} = 26 Torr, balance was He, T = 403 K.

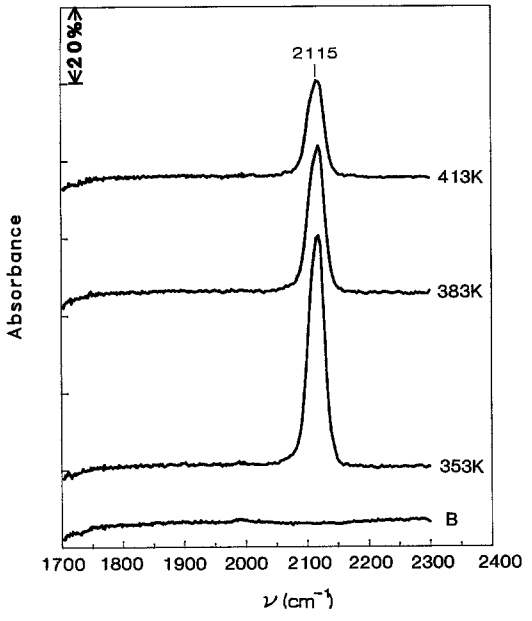

FIG. 7. IR spectra of CO adsorbed on rereduced 12% $Cu/\delta\text{-}Al_2O_3$ (after 3 h in H_2 reduction at 573 K). Gas flow = 28.5 cm^3/min, total pressure = 750 Torr, P_{CO} = 26 Torr, balance was He.

bands have been interpreted as follows: the higher-frequency band above 2100 cm^{-1} is associated with sites on the inner parts of the steps and the lower-frequency band near 2088 cm^{-1} represents terrace sites or those at the outer edge of the steps (*35*). At saturation coverage, the dominant CO bands are 2070 cm^{-1} on the (111) plane, 2088 cm^{-1} on the (100) plane, 2094 cm^{-1} on the (110) plane, and 2105 to 2110 cm^{-1} on the (211), (311), and (755) planes. The low-index planes give significantly lower frequencies than the high-index planes. Hayden *et al.* also studied CO adsorbed on the Cu(111) plane with IR spectroscopy, and in addition to the linearly adsorbed CO band at 2070–2078 cm^{-1}, they were able to observe bridge-bonded CO at 1830 cm^{-1} and physisorbed CO at 2140 cm^{-1} at very low temperatures between 7 and 77 K (*36*).

A number of IR spectroscopic studies of CO adsorbed on supported Cu catalysts have been reported (*21, 37–44*), and a similar variation in the CO band frequency has been observed. It is generally accepted that bands at the highest wavenumber (ca. 2120 cm^{-1}) are associated with less well reduced samples. An exceptionally low value of 2081 cm^{-1} was obtained by Pritchard *et al.* for Cu supported on MgO (*21*), which is quite close to the CO band on the (100) plane, and this was explained by assuming that MgO was crystalline and provided mainly (100) faces on the Cu crystallites due to epitaxial growth on the MgO surface. Other than MgO, the support seems to have a relatively minor effect on the frequency of CO ad-

TABLE 3

IR Adsorption Bands for CO Chemisorbed on Single-Crystal Surfaces of Cu at 77 K[a]

Cu Crystal face	Low coverage (cm^{-1})	High coverage (cm^{-1})
(100)	2079	2088
(111)	2080	2070
(110)	2088, 2104	2094
(211)	2095_w, 2109_m	2110
(311)	2093_m, 2110_m	2093_m, 2104
(755)	2093_w, 2111	2073_m, 2106
Oxidized (111)	2100, 2117	2115
Oxidized (110), 0(2 × 1)	2105	2100, 2137
Oxidized (110), 0(6 × 2)	2113	2110, 2136

Source. References (*26–30, 51*)

[a] m = medium, w = weak.

sorbed on Cu crystallites, and Al_2O_3-supported Cu catalysts have typically given a band near 2109 cm^{-1} (*41, 42*). There is evidence that, in thermodynamic terms, there is little energy difference between the different low-index faces, and it may be that Cu has a greater tendency to form multifaceted crystalline surfaces than do other metals.

Several authors have reported IR spectra of CO adsorbed on CuO, and the band at 2140 cm^{-1}, which can be intense, is assigned to molecularly adsorbed CO (*45–49*). Additional bands range between 1700 and 1100 cm^{-1} and are attributed to bicarbonate, carboxylate, and carbonate species. Few IR spectra of CO adsorbed on Cu_2O have been reported, but both Pearce (*33*) and Hierl *et al.* (*50*) have reported a band close to 2130 cm^{-1}. Hollins and Pritchard (*51*) have reported IR spectra of CO molecules adsorbed on oxidized Cu(111) and Cu(110). At low coverages of CO a doublet at 2100 and 2117 cm^{-1} was obtained for the oxidized Cu(111) plane, while a single band at 2115 cm^{-1} was obtained at higher exposures. For the oxidized Cu(110) plane, a doublet at 2100 and 2140 cm^{-1} existed at higher coverages. Finally, Busca has assigned bands at 2158 and 2115 cm^{-1} to CO adsorbed on Cu^{+2} and Cu^{1+} centers, respectively, on a CuO surface (*52*).

The CO bands obtained in this study are invariant at 2118 cm^{-1}; consequently, we conclude that after our pretreatment these Cu crystallites have residual surface oxygen, as Pritchard *et al.* have proposed (*26*). This conclusion is supported by the fact that the peak position was not changed by the presence of O_2 in the gas stream and by the finding that the initial CO band at 2118 cm^{-1}, which was obtained after the standard 3-h reduction at 573 K, was shifted to 2105 cm^{-1} after an additional reduction of a Pd–Cu/δ-Al_2O_3 catalyst at 573 K for 12 h (*18*). Also, a similar peak position of 2115 cm^{-1} was observed by Smith during this reaction over Cu dispersed on Cabosil (*2*). Since the frequency of this peak (2118 cm^{-1}) is near that of gas-phase CO (2143 cm^{-1}), only a weak bond exists between the O-covered Cu surface and adsorbed CO molecules. In confirmation of this, all the adsorbed CO molecules could be desorbed at 300 K during an overnight purge with He. Based on Busca's assignment (*52*), this CO species at 2118 cm^{-1} is assumed to be adsorbed on Cu^{+1} sites, such as those made available by oxygen vacancies, and the absence of a band near 2158 cm^{-1} indicates the absence of CuO at the surface.

Habraken *et al.* studied intensively the interaction between gas-phase CO molecules and oxygen adsorbed on (100), (110), and (111) single-crystal surfaces, and they measured activation energies of 6–8 kcal/mol for this reaction (*4–7*). They concluded that no major differences existed in the kinetics on these low-index planes, i.e., the reaction was structure insensitive, and that the reaction to form CO_2 proceeded via a L-H mechanism involving adsorbed CO molecules and O atoms, because a decrease in the reaction rate with increasing oxygen coverage was observed and no difference was observed in the reaction rate between surface oxygen originating from O_2 or N_2O, which indicated that O_2 dissociates upon chemisorption. The activation energy for the surface reaction $CO_{ad} + O_{ad} \rightarrow CO_2$ was estimated to be between 18 and 20 kcal/mol for all three planes based on a heat of adsorption of 12 kcal/mol for CO on copper (*7*). Ertl observed a deactivation of the catalyst after a longer interaction with oxygen, and he also proposed a reaction between adsorbed reactants (*3*). Miro *et al.* reported an apparent activation energy of 12 kcal/mol for a CuO/mordenite catalyst (*13*), while over silica-supported CuO catalysts, De Jong *et al.* (*49*) reported an activation energy of 15 kcal/mol and Prokopowicz *et al.* (*10*) obtained an activation energy of 14.1 kcal/mol, but the latter authors proposed an Eley–Rideal reaction mechanism for the CO oxidation reaction. However, the Cu oxide phase actually present was not determined in either of the last two studies. In contrast, Russian authors have reported a low activa-

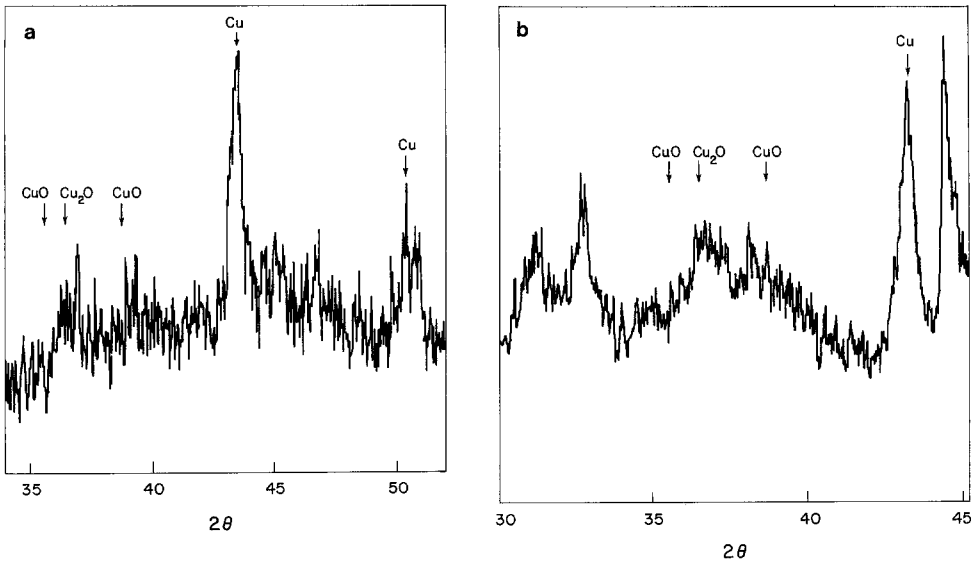

FIG. 8. (a) XRD pattern of reduced 12% Cu/δ-Al_2O_3 after H_2 and CO chemisorption (no air exposure). (b) XRD pattern of reduced 12% Cu/δ-Al_2O_3 catalyst in (a) after exposure to air.

tion energy near 7 kcal/mol over unsupported CuO catalysts (*53, 54*). For bulk Cu_2O, Garner *et al.* reported an activation energy of 11.4 kcal/mol (*16*).

The state of the surface of these Cu particles under steady-state reaction conditions is not precisely known; however, on the Cu crystallites in our study it is presumed to be composed of a very thin layer of Cu oxide with a stoichiometry very near that of Cu_2O. This picture is based upon the following information. First, oxygen uptakes under 200 Torr O_2 on SiO_2-supported Cu at temperatures of 350–400 K indicate that only two to three monolayers of Cu_2O are formed. (*55*). Second, the XRD powder patterns in Fig. 8 show that only Cu^0 is visible after reduction and CO chemisorption, and even after extensive air exposure, little Cu oxide formation is detected and the particles remain predominantly as metallic Cu. This is consistent with the work of Severino *et al.* who found primarily Cu^0 XRD peaks after oxidation of 5–30% Cu/Al_2O_3 catalysts at 473 K (*56*). Third, the ease of reducibility of Cu oxides, especially CuO, by CO is well established (*13, 56*), and this would control the depth of this oxide film under reaction conditions. Finally, the 2118 cm^{-1} band for CO is consistent with that expected for adsorption on Cu_2O (*52*). Consequently, our visualization of the surface under reaction conditions is that of a near-stoichiometric layer of Cu_2O on metallic Cu, perhaps two to three monolayers thick, with oxygen vacancies exposing Cu^{1+} sites, or possibly Cu_2O/Cu^0 interfacial sites as proposed by Miro *et al.* (*13*), upon which CO can adsorb. Such a model is consistent with the IR spectra obtained in this study and with previous observations indicating the absence of CuO (*57*). The apparent activation energies of 17–22 kcal/mol determined in Fig. 1 at the low-temperature reaction conditions used here are somewhat higher than most previous values, whether they pertain to metallic Cu surfaces or (at least initially) CuO and Cu_2O surfaces.

Compared to prereduced Al_2O_3-supported Pd operating at the standard reaction conditions employed here (P_{O_2} = 132 Torr, P_{CO} = 26 Torr), the TOFs are two to eight times higher than the range of TOFs reported for these Pd catalysts (*17*). However,

the *average* TOF on Cu is only three to four times greater than the average TOF on Pd and the assumption of an adsorption stoichiometry of $CO/Cu_s = 0.5$ would make the average TOFs on these two metals quite similar. It should be stressed that at different reactant partial pressures a much greater spread in TOFs could easily occur because of the significant difference in pressure dependencies; i.e., the rate expression is $r = kP_{CO}^{0.7} P_{O_2}^{0}$ on copper while it is near $r = kP_{CO}^{-0.5} P_{O_2}^{1}$ on Pd at lower O_2 pressures (*18*).

Since this study found a small increase in activity with decreasing oxygen partial pressure, i.e., decreasing oxygen coverage, in agreement with UHV studies (*3–8*), and the activity showed a near-first-order dependence on CO pressure, a L-H mechanism was strongly indicated. It is well known that O_2 adsorbs dissociatively and strongly on Cu [the heat of adsorption of O_2 is 50 kcal/mol (*3*)]; therefore, high coverages of adsorbed oxygen atoms might be anticipated. If CO molecules on the surface are reactive intermediates, it can be assumed that a surface reaction between adsorbed CO and oxygen atoms occurs and, if this is the rate-determining step (RDS), the reaction rate can be expressed as follows:

$$r = k\theta_{CO}\theta_O. \qquad (1)$$

During the CO partial pressure dependency run, if θ_O is considered nearly constant because the oxygen partial pressure was not varied, then a plot of the activity versus the absorbance of the 2118 cm^{-1} band will show the dependency of the rate on the coverage of adsorbed CO. Indeed, as shown in Fig. 9, a first-order dependency on chemisorbed CO was obtained. Furthermore, a similar first-order plot was obtained from the CO spectra taken during the oxygen partial pressure run (*58*). If it is assumed that O coverages remain high and thus vary little, then any change in activity should again correlate with the concentration of adsorbed CO. This assumption is supported by the fact that the amount of CO adsorbed on the surface did not change markedly (ca. 15–20%) even

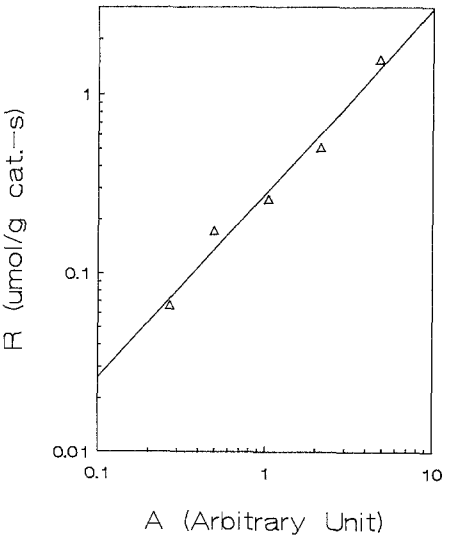

FIG. 9. Dependence of the rate of CO oxidation on CO surface coverage as indicated by the absorbance of the 2118 cm^{-1} band on 12% Cu/δ-Al_2O_3. P_{O_2} = 132 Torr, T = 403 K.

though the oxygen pressure was varied from 84 to 16 Torr. The near-first-order dependency on CO coverage provides further support for the L-H model proposed by previous workers (*4–8*), and it extends the range of applicability to much higher CO pressures.

To derive a rate expression based on a standard L-H model, the normal assumptions were made; i.e., CO and oxygen adsorb as molecules and atoms, respectively, and the surface reaction between adsorbed CO molecules and oxygen atoms to produce CO_2 represents the RDS (*7*). The following rate expression can be readily obtained:

$$r = k\frac{K_{CO}P_{CO}\sqrt{K_{O_2}P_{O_2}}}{(1 + K_{CO}P_{CO} + \sqrt{K_{O_2}P_{O_2}})^2}. \qquad (2)$$

Equation (2) was derived with the assumption that CO and oxygen compete for adsorption on the same surface sites, i.e., on metallic Cu, and this can produce inhibited CO adsorption at high surface coverages of oxygen, that is, when the $K_{O_2}P_{O_2}$ term in the denominator dominates. However, once an

TABLE 4

Computed Rate Parameters (k, K_{CO}, and K_{O_2}) at 403 K for Prereduced 12% Cu/δ-Al_2O_3

Rate expression	Constant		
	k (s^{-1})	K_{CO}[a]	K_{O_2}[a]
Eq. (2): competitive adsorption on Cu^0	5.6	59	110
Eq. (5): noncompetitive adsorption	1.7	32	9.8×10^4

[a] Based on units of atm^{-1} and a standard state of 1 atm.

oxide layer has been formed on the surface, CO adsorption appears to have little dependence on the oxygen pressure, as shown in Fig. 6. Consequently, the sites available for CO on this surface may be different from those able to dissociatively chemisorb an O_2 molecule; for example, CO may adsorb on a Cu^{1+} cation at an O vacancy, and this situation would result in an absence of competitive adsorption between CO and oxygen. Then two independent Langmuir isotherms can be written for nondissociative CO adsorption and dissociative O_2 adsorption, i.e.,

$$\theta_{CO} = \frac{K_{CO}P_{CO}}{1 + K_{CO}P_{CO}} \tag{2}$$

$$\theta_O = \frac{\sqrt{K_{O_2}P_{O_2}}}{1 + \sqrt{K_{O_2}P_{O_2}}}, \tag{4}$$

and substitution of Eqs. (3) and (4) into Eq. (1) gives the following L-H rate expression:

$$r = \frac{kK_{CO}K_{O_2}^{1/2}P_{CO}P_{O_2}^{1/2}}{(1 + K_{CO}P_{CO})(1 + K_{O_2}^{1/2}P_{O_2}^{1/2})}. \tag{5}$$

Using a direct search simplex method, the constants k, K_{CO}, and K_{O_2} in Eqs. (2) and (5) were computed which gave the optimum fit of these equations to the partial pressure data. The values of these constants are listed in Table 4 and the predicted behavior from Eq. (5) is compared with the data in Fig. 2.

Since partial pressure dependencies on the reactants were obtained at only one temperature, it is not possible to calculate entropies and enthalpies of adsorption and to evaluate their physical consistency. However, from IR spectra such as those in Fig. 4, the heat of adsorption for CO on this catalyst under reaction conditions can be estimated. The CO coverage from the Langmuir isotherm θ_{CO} is given by Eq. (3) where K_{CO} is the equilibrium adsorption constant. At low coverage, $K_{CO}P_{CO} \ll 1$; therefore,

$$\theta_{CO} \cong KP_{CO}. \tag{6}$$

For an adsorbed species, the absorbance in an IR spectrum is proportional to the surface concentration; hence

$$\theta = A/A_o \tag{7}$$

where A is the absorbance at any coverage and A_o is that at saturation coverage. The equilibrium constant can be represented in terms of the enthalpy and entropy of adsorption, i.e.,

$$K = \exp\left(\frac{\Delta S_{ad}^o}{R}\right)\exp\left(\frac{-\Delta H_{ad}^o}{RT}\right). \tag{8}$$

Substituting Eqs. (7) and (8) into (6), taking the logarithm of each side, and rearranging give the equation

$$\ln A = \frac{-\Delta H_{ad}^o}{R}\left(\frac{1}{T}\right) + \left(\frac{\Delta S_{ad}^o}{R} + \ln P_{CO} + \ln A_o\right). \tag{9}$$

Therefore, a graph of $\ln A$ versus $1/T$ at constant P_{CO} enables one to calculate

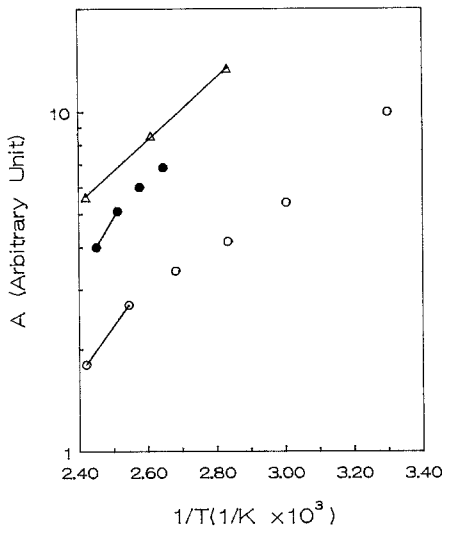

FIG. 10. Dependence of the CO surface coverage on temperature as monitored by the absorbance of the 2118 cm^{-1} band on 12% Cu/δ-Al_2O_3. P_{CO} = 26 Torr, P_{O_2} = 132 Torr. ○, Ascending temperature (Fig. 4); ●, descending temperature (Ref. *58*); △, obtained in He only (Ref. *58*).

ΔH°_{ad}, and these plots are shown in Fig. 10. With CO in He, the heat of adsorption of CO was about 4.2 kcal/mol on these incompletely reduced surfaces, and during the partial pressure runs the heat of adsorption of CO was between 3.6 and 5.4 kcal/mol over the lower-temperature region. However, if the slope is evaluated in the temperature range around 403 K, at which temperature the partial pressure runs were conducted, an average value of 7.2 ± 0.7 kcal/mol is obtained for $-\Delta H^0_{ad}$ ($-\Delta H^0_{ad} = Q_{ad}$). This latter value is not significantly different than those reported for CO on copper surfaces with relatively high CO coverages ($\theta = \frac{1}{2}$ or greater), which range from 7 to 10 kcal/mol (*59–61*). With this value it is possible to estimate minimum and maximum values for ΔS^0_{ad} (*62, 63*) by using the expression

$$10 \leq -\Delta S^\circ_{ad} \leq 12.2 - 0.0014(-\Delta H^\circ_{ad}), \quad (10)$$

and this gives a range of reasonable values for K_{CO} which fall between 0.5 and 50 atm^{-1}. The values from the computer-derived constants in Eqs. (2) and (5) are 59 and 32, respectively, as shown in Table 4; consequently, both are acceptable within the uncertainty involved, although the K_{CO} value of 32 from the noncompetitive adsorption model appears more appropriate. The much higher K_{O_2} value from this latter model is also more consistent with our results and previous studies showing that oxygen adsorbs much more strongly than CO on copper surfaces. The similarity in K_{CO} and K_{O_2} values obtained from Eq. (2) would imply similar coverages. Finally, a slightly better fit of the kinetic data for the O_2 dependence in Fig. 2 is obtained with Eq. (5), but Eqs. (2) and (5) give similar fits for the CO dependence. Strong, immobile adsorption of a diatomic molecule requiring two sites can produce a low concentration (ca. 8–9%) of vacant single sites in the monolayer coverage (*64, 65*). If metallic Cu atoms are present at the surface, it could be these vacant sites that adsorb CO. Alternatively, if only Cu^{1+} sites were present the noncompetitive adsorption model would better describe this situation, and this could be why it appears more appropriate to use. We cannot make a distinction between these possibilities with our data but favor the latter.

An effort was also made to estimate an activation energy for the rate-determining step, which is the reaction between adsorbed CO molecules and oxygen atoms. The $K_{CO}P_{CO}$ term in the denominator in either Eq. (2) or (5) is not negligible and is on the order of unity because of the 0.7 order dependence. This complicates any estimate of an activation energy; however, it was observed that the dependency on O_2 was near zero, and thus a reasonable approximation is

$$r = k(K_{CO}P_{CO})^{0.7}. \quad (11)$$

Therefore,

$$E_{app} = E - 0.7Q_{CO} \quad (12)$$

where E_{app} is the apparent activation energy, E is the activation energy for the RDS, and

Q_{CO} is the heat of adsorption for CO on this O-covered copper surface. The measured E_{app} values varied from 17 to 22 kcal/mol and the Q_{CO} value from the IR spectra was 7.2 kcal/mol; therefore, the activation energy for the surface reaction between an adsorbed CO molecule and an adsorbed O atom lies between 22 and 27 kcal/mol. This range is somewhat larger than the reported values of 18–20 kcal/mol for CO reacting with less than a monolayer of chemisorbed oxygen on metallic Cu single-crystal surfaces under UHV conditions (*4–7*), but it is quite consistent with a value of 25 kcal/mol reported for this kinetic step on Pd (*66*). The more extensive surface oxidation that should occur under these high O_2 pressures can explain the difference in the activation energy compared to that for oxygen on copper single crystals.

SUMMARY

A kinetic study of the CO oxidation reaction over supported, prereduced Cu crystallites showed that it is close to first order in CO and near zero order in O_2 at temperatures around 400 K. *In situ* IR measurements under reaction conditions revealed a clear first-order dependence on chemisorbed CO and an absence of activity when no adsorbed CO was detected. Thus an Eley–Rideal mechanism can be eliminated and a Langmuir–Hinshelwood surface reaction between adsorbed CO molecules and O atoms is strongly supported. These Cu/Al_2O_3 catalysts are more active than Pd/Al_2O_3 catalysts and TOFs were up to five times higher at 400 K than those for Pd.

Oxygen adsorbs much more strongly than CO on copper, and therefore CO adsorption can be decreased on these Cu surfaces that are nearly saturated with chemisorbed O atoms. XRD patterns showed the presence of only Cu metal after reduction while primarily metallic Cu with a small detectable amount of Cu_2O could be observed after air exposure. No CuO was detected. A L-H sequence invoking noncompetitive adsorption between O_2 and CO on these O-covered surfaces appears to be more appropriate than a L–H sequence assuming competitive adsorption. Consequently, one model of this system would propose that the surface of these particles may exist as a thin overlayer (two to three monolayers) of Cu_2O with O vacancies, allowing CO adsorption on exposed Cu^{+1} sites, or possibly on Cu_2O/Cu interface sites, while O_2 would interact with metallic surface Cu atoms to maintain this Cu_2O layer. Analysis of the rate parameters from either L-H rate expression indicated they were reasonable, and the IR spectra at various temperatures allowed a heat of adsorption of 7.2 kcal/mol to be estimated for CO under reaction conditions. The use of this value and the apparent activation energies of 17–22 kcal/mol indicated a range of 22–27 kcal/mol for the rate-determining step, which was somewhat higher than the values of 18–20 kcal/mol reported for CO and oxygen on Cu single crystals but very consistent with the value of 25 kcal/mol reported for CO and oxygen on Pd.

ACKNOWLEDGMENTS

This research was sponsored by a grant from Teledyne Water Pik, Fort Collins, Colorado. Additional support was provided by the Mobil Research and Development Corporation.

REFERENCES

1. Jones, H. A., and Taylor, H. S., *J. Phys. Chem.* **27,** 623 (1923).
2. Smith, A. W., *J. Catal.* **4,** 172 (1965).
3. Ertl, G., *Surf. Sci.* **7,** 309 (1967).
4. Habraken, F. P. H. M., Keifer, E. Ph., and Bootsma, G. A., *Surf. Sci.* **83,** 45 (1979).
5. Habraken, F. P. H. M., and Bootsma, G. A., *Surf. Sci.* **87,** 333 (1979).
6. Habraken, F. P. H. M., Bootsma, G. A., Hofman, P., Hachicha, S., and Bradshaw, A. M., *Surf. Sci.* **88,** 285 (1979).
7. Habraken, F. P. H. M., Mesters, C. M. A. M., and Bootsma, G. A., *Surf. Sci.* **97,** 264 (1980).
8. Arlow, J. S., and Woodruff, D. P., *Surf. Sci.* **180,** 89 (1987).
9. Kummer, J. T., *Prog. Energy Combust. Sci.* **6,** 177 (1980).
10. Prokopowicz, R. A., Silveston, P. L., Hudgins, R. R., and Irish, D. E., *React. Kinet. Catal. Lett.* **37,** 63 (1988).
11. Liao, P. C., Carberry, J. J., Fleisch, T. H., and Wolf, E. E., *J. Catal.* **74,** 307 (1982).

12. Schwab, G. M., and Drikes, A., *Z. Phys. Chem. B* **52,** 234 (1942).
13. Miro, E. E., Lombardo, E. A., and Petunchi, J. O., *J. Catal.* **104,** 176 (1987).
14. Huang, T-J., Yu, T-C., and Chang, S-H., *Appl. Catal.* **52,** 157 (1989).
15. Garner, W. E., Gray, T. J., and Stone, F. S., *Proc. R. Soc. A* **197,** 294 (1949).
16. Garner, W. E., Stone, F. S., and Tiley, P. F., *Proc. R. Soc. A* **221,** 472 (1952).
17. Choi, K. I., and Vannice, *J. Catal.,* **131,** 1 (1991).
18. Choi, K. I., and Vannice, *J. Catal.,* **131,** 36 (1991).
19. Palmer, M. B., and Vannice, M. A., *J. Chem. Technol. Biotechnol.* **30,** 205 (1986).
20. Choi, K. I., and Vannice, M. A., *J. Catal.* **127,** 465 (1991).
21. Chesters, M. A., and Pritchard, J., *Surf. Sci.* **28,** 460 (1971).
22. Wolberg, A., and Roth, J. F., *J. Catal.* **15,** 250 (1969).
23. Wolberg, A., Ogilvie, J. L., and Roth, J. F., *J. Catal.* **19,** 86 (1970).
24. Friedman, R. M., and Freeman, J. J., *J. Chem. Soc. Trans. Faraday 1,* 758 (1978).
25. Friedman, R. M., Freeman, J. J., and Lytle, F. W., *J. Catal.* **55,** 10 (1978).
26. Chesters, M. A., Pritchard, J., and Sims, M. L., *Chem. Commun.,* 1454 (1970).
27. Pritchard, J., *J. Vac. Sci. Technol.* **9,** 895 (1972).
28. Pritchard, J., Catterick, T., and Gupta, R. K., *Surf. Sci.* **53,** 1 (1975).
29. Horn, K., and Pritchard, J., *Surf. Sci.* **55,** 701 (1976).
30. Horn, K., Hussain, M., and Pritchard, J., *Surf. Sci.* **63,** 244 (1977).
31. Pritchard, J., *Surf. Sci.* **79,** 231 (1979).
32. Hollins, P., and Pritchard, J., *Surf. Sci.* **89,** 486 (1979).
33. Pearce, H. A., Ph.D. thesis, University of East Anglia, Norwich, 1974.
34. Grimley, T. B., *Proc. Phys. Soc. London* **90,** 751 (1967).
35. Sheppard, N., and Nguyen, T. T., *Adv. Infrared Raman Spectrosc.* **5,** 67 (1978).
36. Hayden, B. E., Kretzschmar, K., and Bradshaw, A. M., *Surf. Sci.* **155,** 553 (1985).
37. Eischens, R. P., Pliskin, W. A., and Francis, S. A., *J. Chem. Phys.* **22,** 1786 (1954).
38. Eischens, R. P., and Pliskin, W. A., *Adv. Catal.* **10,** 1 (1958).
39. Kavtaradze, N. N., and Sokolova, N. P., *Dokl. Phys. Chem.* **146,** 747 (1962).
40. Kavtaradze, N. N., and Sokolova, N. P., *Russ. J. Phys. Chem.* **44,** 603 (1970).
41. Kavtaradze, N. N., and Sokolova, N. P., *Dokl. Phys. Chem.* **172,** 39 (1967).
42. Smith, A. W., and Quets, J. M., *J. Catal.* **4,** 163 (1965).
43. Cho, J. S., and Schulman, J. H., *Surf. Sci.* **2,** 245 (1964).
44. Cukr, N., *Chem. Listy* **64,** 785 (1970).
45. London, J. W., and Bell, A. T., *J. Catal.* **31,** 32 (1973).
46. Gardner, R. A., and Petrucci, R. H., *J. Am. Chem. Soc.* **82,** 5051 (1965).
47. Seanor, D. A., and Amberg, C. H., *J. Chem. Phys.* **42,** 2967 (1965).
48. Davydov, A. A., Rubene, N. A., and Budneva, A. A., *Kinet. Katal.* **19,** 776 (1978).
49. De Jong, K. P., Geus, J. W., and Joziasse, J., *J. Catal.* **65,** 437 (1980).
50. Hierl, R., Knozinger, H., and Urbach, H. P., *J. Catal.* **69,** 475 (1981).
51. Hollins, P., and Pritchard, J., *Surf. Sci.* **134,** 91 (1983).
52. Busca, G., *J. Mol. Catal.* **43,** 225 (1987).
53. Boreskov, G. K., and Marshneva, V. I., *Dokl. Akad. Nauk SSSR* **213,** 112 (1973).
54. Vorontsov, A. V., Kasatkina, L. A., Dzisyak, A. P., and S. V. Tikhonova, *Kinet. Katal.* **20,** 1194 (1979).
55. Leon y Leon, C. A., and Vannice, M. A., *Appl. Catal.,* **69,** 269 (1991).
56. Severino, F., Brito, J., Carias, O., and Laine, J., *J. Catal.* **102,** 172 (1986).
57. Giamello, E., Fubini, B., Lauro, P., and Bossi, A., *J. Catal.* **87,** 443 (1984).
58. Choi, K. I., Ph.D. thesis, Pennsylvania State University, 1990.
59. Harendt, C., Goschnick, J., and Hirschwald, W., *Surf. Sci.* **152/153,** 453 (1985).
60. Horn, K., Hussain, M., and Pritchard, J., *Surf. Sci.* **63,** 244 (1977).
61. Kessler, J., and Thieme, F., *Surf. Sci.* **67,** 405 (1977).
62. Boudart, M., Mears, D. E., and Vannice, M. A., *Ind. Chem. Belg.* **32,** 281 (1967).
63. Vannice, M. A., Hyun, S. H., Kalpakci, B., and Liauh, W. C., *J. Catal.* **56,** 358 (1979).
64. Miller, A. R., "Chemisorption of Gases on the Solids," p. 55. Cambridge Press, London, 1948.
65. Rossington, D. R., and Borst, E., *Surf. Sci.* **3,** 202 (1965).
66. Engel, T., and Ertl, G., *Adv. Catal.* **28,** 1 (1979).